J6.1 DISTRIBUTION AND VARIABILITY OF ATMOSPHERIC TEMPERATURE AND WATER VAPOR DERIVED FROM HIRS MEASUREMENT

Lei Shi * and John J. Bates
NOAA National Climatic Data Center, Asheville, North Carolina

1. INTRODUCTION

The High Resolution Infrared Radiation Sounder (HIRS) is one of the primary instruments on board the National Oceanic and Atmospheric Administration (NOAA) polar orbiting satellite series. The sounder provides routine measurement of the atmosphere on a global scale. It has twenty spectral channels, twelve of which are longwave channels. Among the longwave channels, channels 1-7 are located in the carbon dioxide absorption band. Channel 8 is a window channel. Channel 9 is in the ozone band. Channel 10 is in the water vapor continuum band. Channels 11 and 12 are water vapor sensitive. The channel frequencies are carefully selected to sound different levels of the atmosphere from the surface to the stratosphere.

A time series of cloud-cleared HIRS dataset has been generated by Jackson and Bates (2001). As the HIRS instrument has been carried on each of the NOAA satellite series since TIROS-N, the data were adjusted to a baseline instrument based on NOAA-10 to avoid spurious jumps in the time series due to changes in channel filter functions and differences in satellite equator crossing time. Significant work has been accomplished using this inter-satellite calibrated HIRS dataset. For example, Bates and Jackson (2001) and Bates et al. (2001) examined the variability of upper tropospheric humidity. The studies showed that while the interannual variability of spatial fields was dominated by the major El Niño events, the upper tropospheric humidity exhibited more prominent seasonal variation.

The current study derives temperature and water vapor profiles at different levels of the atmosphere, and examines the horizontal and vertical distribution and variability of these variables. A neural network technique is used to develop the retrieval scheme which connects the non-linear relationship between the retrieved variables and the HIRS channel brightness temperature.

2. NEURAL NETWORK RETRIEVAL

The neural network dataset represents the matched patterns of the atmospheric profiles and the HIRS channel brightness temperature. The profiles are obtained from a diverse sample of profiles simulated by the European Center for Medium-Range Weather Forecasts (ECMWF) system (Chevallier, 2001). These profiles are selected from the first and the 15th of each month between January 1992 and December 1993. The profiles are divided into seven groups differing by the total precipitable water vapor content of the profiles. About the same number of samples are extracted from each group, except for the group with the lowest precipitable water vapor content (0 to 0.5 $kg.m^{-2}$). For this group, twice as many profiles are extracted in consideration of the higher temperature variability from all types of situations from polar to tropics. The corresponding HIRS channel brightness temperatures are simulated by a radiative transfer model, RTTOV7. The RTTOV is a broadband model in that the integration over the channel response is simulated directly. A description of the RTTOV can be found in Saunders et al. (1999). The RTTOV was one of the participating models in an intercomparison of HIRS and AMSU channel radiance computation (Garand et al., 2001). Among the selected seven HIRS channels (channels 2, 5, 9, 10, 11, 12, and 15) examined in the intercomparison, the standard deviations of RTTOV simulated radiances are within 0.25 K for the five non water vapor channels, and within 0.55 K for the two water vapor channels.

Backpropagation neural networks similar to the approach used by Shi (2001) are used in developing the retrieval scheme. Different architectures with different numbers of layers and transfer functions are examined for the temperature and water vapor profiles retrieval. A five-layer network, with one input layer, three hidden layers, and one output layer, is chosen based on the improved performance compared to four-layer and three-layer networks. It is found that using a hyperbolic tangent function to propagate to each of the three hidden layers and a logistic transfer function to propagate to the output layers gives the optimum network performance for the type of data studied. The definition of the hyperbolic tangent transfer function is

$$f(x) = \tanh(x), \quad (1)$$

and the definition of the logistic transfer function is

$$f(x) = \frac{1}{1+\exp(-x)}. \quad (2)$$

The input set includes the twelve HIRS longwave channels. The retrieval temperatures are obtained at 18 pressure levels from 1005 hPa to 50 hPa, and the water vapor mixing ratios are obtained at 13 levels from 1005 hPa to 300 hPa.

Because the neural network training dataset requires values at each pressure level, the training profiles with the surface pressure value less than 975 hPa are excluded. This builds a total of 9978 collocated patterns. Among these patterns, 20% (1955 patterns) are randomly extracted to construct a testing set, and another 20% are randomly extracted and set aside as a validation set for

* *Corresponding author address*: Lei Shi, National Climatic Data Center, 151 Patton Avenue, Asheville, NC 28801; e-mail: lei.shi@noaa.gov.

later statistical studies. As a result, there are 5988 patterns remaining and they are kept in the learning set. A backpropagation network is trained by "supervised learning". The network is presented with a series of pattern pairs, each consisting of an input pattern and an output pattern, in random order until predetermined convergence criteria are met. At this time the network presents the input elements in the testing set and retrieves the output elements. Then the retrieved output elements are compared with the output elements in the testing set, and the averaged root mean square error (RMSE) of all the output elements is computed. The network parameters are saved if the averaged RMSE is less than that computed previously. This process is repeated until no improvement is found for a specified number of test trials.

The saved neural network parameters are applied to the data in the validation dataset. The RMSEs of temperature and water vapor mixing ratio at all the levels are derived assuming the outputs in the validation database as truth data. For temperature, the RMSEs are about 2°C at the near-surface levels, 1.1-1.2°C in the mid troposphere, and about 2°C around the tropopause and in the lower stratosphere. For water vapor, the RMSE is 1.9 g/kg at 1005 hPa. It steadily decreases to 1.1 g/kg at 700 hPa and less than 0.5 g/kg above 500 hPa.

3. DERIVED TEMPERATURE AND WATER VAPOR

Using the saved neural network models, temperature and water vapor profiles are computed based on eighteen years (1979-1996) of HIRS channel brightness temperatures. As an example of the horizontal temperature distribution, Fig. 1 shows the mean temperature at 1005 hPa from 70°N to 70°S. The HIRS retrieval provides global coverage of temperature profiles except the regions where permanent snow/ice cover cannot be easily distinguished from the clouds. The coverage includes oceans and many of the remote regions that are not observed by conventional radiosondes. Fig. 1 shows that the temperature distribution follows closely the distribution of solar radiation. The highest temperatures are located in the tropics with maximums in the western Pacific and the Indian oceans. The lowest temperatures are found in the high latitudes. The temperature gradients are very small in the equatorial regions. The strongest zonal gradients are formed along the mid-latitudes. There is a large land-sea temperature contrast. The temperature across the coast lines often differ more than 10°C. The temperatures are significantly lower over the mountain regions such as the Rocky Mountains in North America and the Andes in South America.

To show the variability of temperature, the standard deviation (STD) values of temperature at 1005 hPa are computed and illustrated in Fig. 2. The smallest values of STDs are seen in the equatorial oceanic regions due to small seasonal variation of temperature. The largest STD values are located in mid and high latitudes in the northern hemisphere as a result of frequent frontal activities. At a same latitude, the temperature variability over land is significantly larger than over the ocean. The largest STD values are centered in the Siberia where there are frequent frontal generations and passages which produce large seasonal temperature variations.

Fig. 3 shows the eighteen-year mean distribution of water vapor mixing ratio at 1005 hPa. The highest values are found over the equatorial western Pacific and the Indian Oceans. The influence of land effect on the distribution of water vapor is apparent. At a same latitude, water vapor mixing ratios over land are lower than over the ocean. Large tropical islands, especially the Indonesian archipelago, exhibit remarkably lower water vapor than the surrounding oceans. The variability of water vapor mixing ratio is shown in Fig. 4. Though the equatorial oceanic regions have high values of mixing ratio, the STDs in these regions are very small. In contrast, the STDs over land surfaces are generally higher. The highest STD values are located in mid latitudes, with much higher values in the Northern Hemisphere than in the Southern Hemisphere. The maximums are centered between 30-40°N in the areas associated with frequent large scale weather systems.

The HIRS retrievals provide vertical structures of atmospheric temperature and water vapor. The zonal mean and STD of temperature are given in Figs. 5 and 6. Fig.5 shows that temperature decreases steadily with height in the stratosphere and increases slightly with height in the lower stratosphere. Comparing the northern and southern latitudes, the mean tropospheric temperatures in the Northern Hemisphere are slightly warmer than the same latitudes in the Southern Hemisphere. The variability of temperature (Fig. 6) is large in the lower troposphere over high latitudes and small in mid to upper troposphere over the tropics. The low temperature and large STD values near 50 hPa level in the high latitude of the southern hemisphere indicate the location of the Antarctic jet.

The zonal mean and STD of water vapor mixing ratio are given in Figs. 7 and 8. As expected, the highest water vapor content is found near surface level in the tropics. The water vapor decreases toward high latitudes and with height. The northern hemisphere has larger water vapor content than over the same latitudes in the southern hemisphere. The STDs (Fig. 8) are large in the lower troposphere and decrease toward the top of the atmosphere with the decrease of water vapor in high altitude. The maximum values are found in mid latitudes due to frequent frontal activities. The variability is more significant in the Northern Hemisphere.

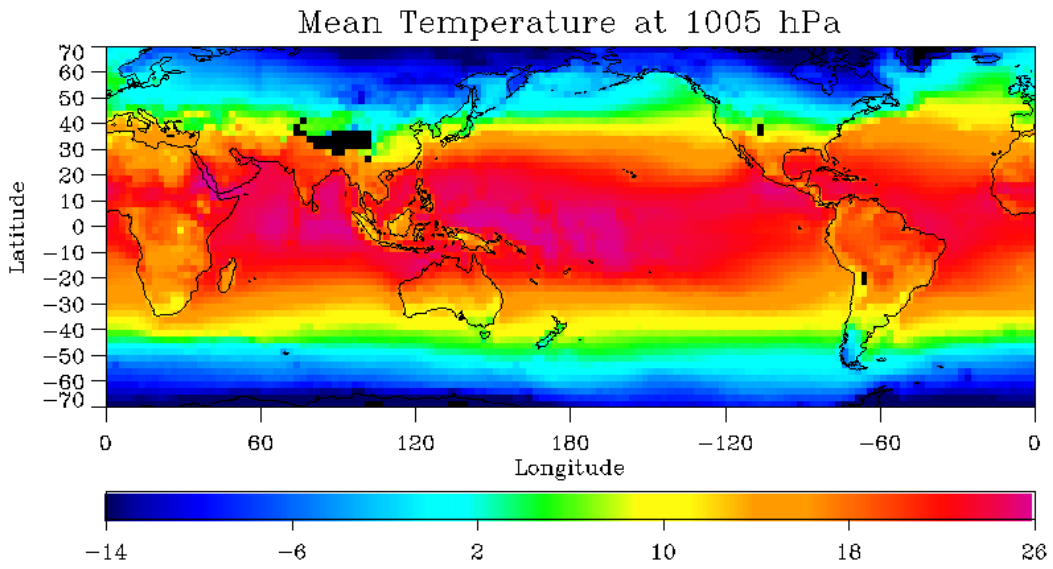

Figure 1. Distribution of temperature at 1005 hPa.

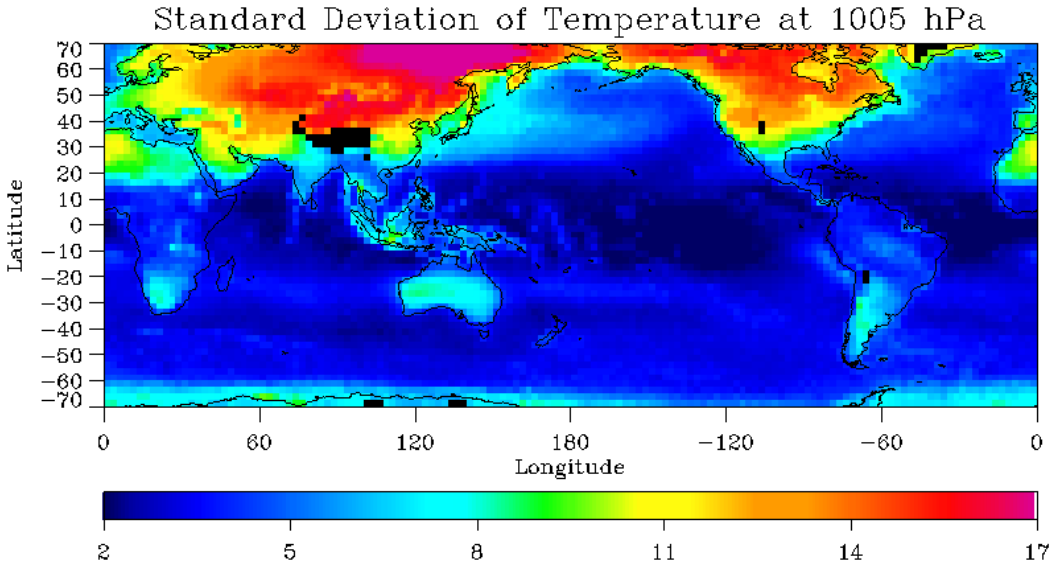

Figure 2. Standard deviation of temperature at 1005 hPa.

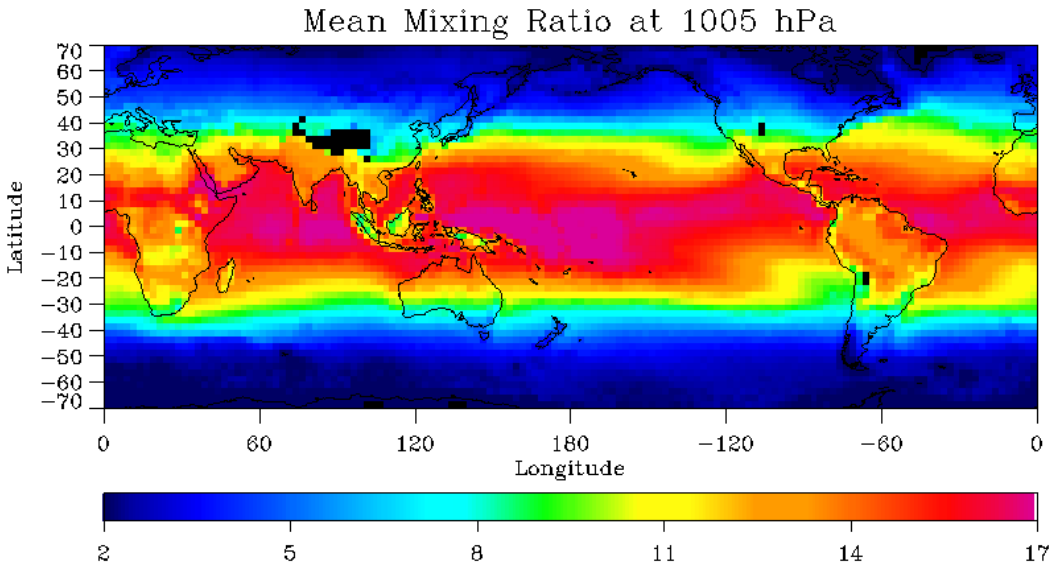

Figure 3. Distribution of water vapor mixing ratio at 1005 hPa.

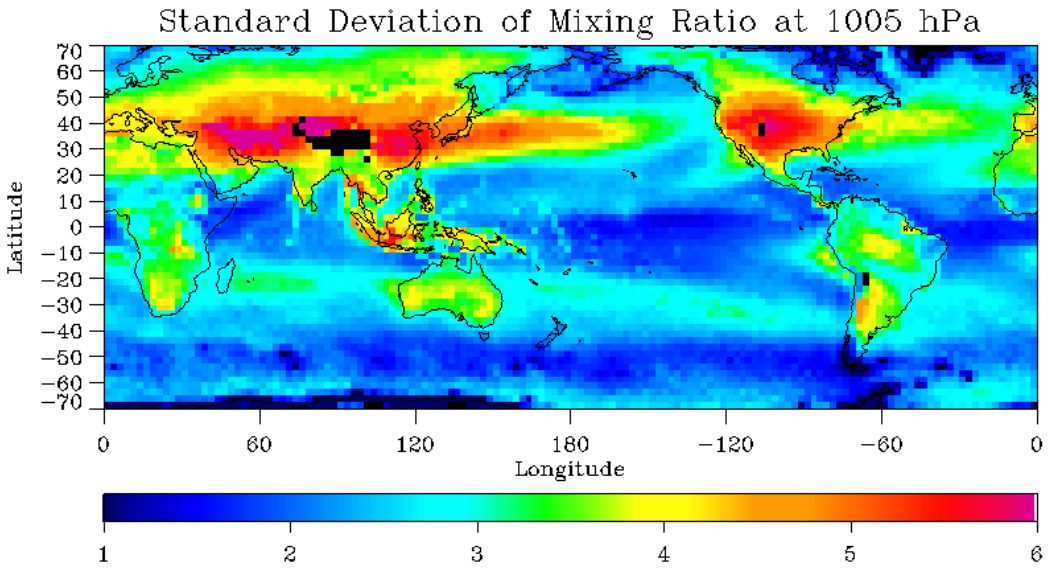

Figure 4. Standard deviation of water vapor mixing ratio at 1005 hPa.

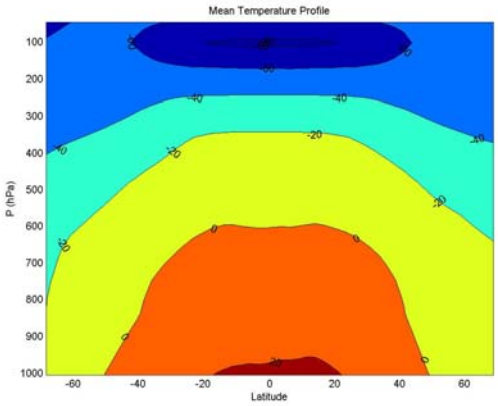

Figure 5. Zonal mean cross sections of the temperature (ºC).

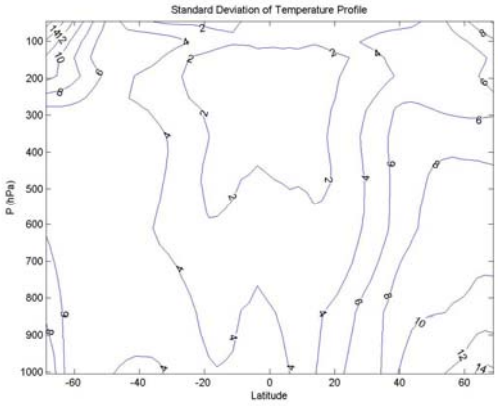

Figure 6. Zonal cross sections of the standard deviation of temperature (ºC).

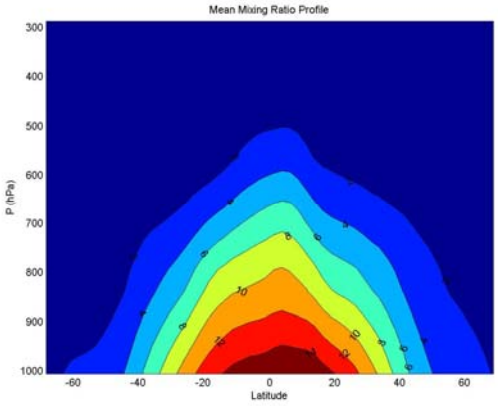

Figure 7. Zonal mean cross sections of the water vapor mixing ratio (g/kg).

4. SUMMARY AND CONCLUSION

A neural network technique is used to derive temperature and water vapor profiles based on HIRS measurement. Sampled profiles from ECMWF representing the global atmospheric conditions are used as the training dataset. It is found that five-layer backpropagation neural networks with proper transfer functions are well suited for the retrievals.

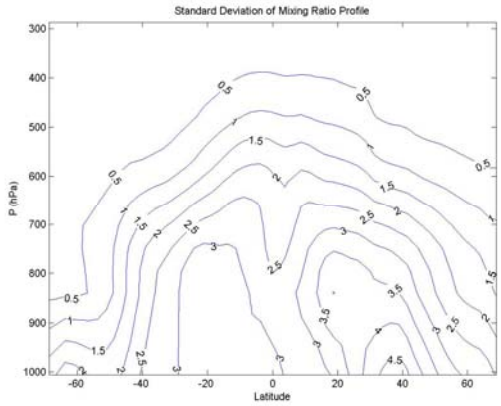

Figure 8. Zonal cross sections of the standard deviation of water vapor mixing ratio (g/kg).

The retrieval schemes are applied to inter-satellite calibrated HIRS measurement between 70ºN and 70ºS. The HIRS measurement provides uniformed coverage through the entire region, including the vast ocean surface and remote mountainous regions that are not completely covered by conventional radiosondes. By computing the STD distributions, the results reveal detailed variabilities of the temperature and water vapor. Over the equatorial region between 20ºN and 20ºS where the temperature and water vapor are largest, the STD plots show very different characteristics of variability between the ocean and land surfaces. The variabilities of both temperature and water vapor over the equatorial ocean areas are very small. In contrast, significant variabilities are found over the land surfaces. The mid latitudes exhibit the largest gradients of both temperature and water vapor. The varibilities are high largely due to frontal weather systems. In the zonal mean vertical sections, the largest variabilities of both temperature and water vapor are found in the mid latitudes, more significantly in the Northern Hemisphere. In the southern high latitude around 50 hPa, the existence of the Antarctic jet results in a highly variable temperature field.

The examples discussed here demonstrate the use of HIRS measurement to examine the distribution and variability of temperature and water vapor in the atmosphere. The HIRS instrument has provided the longest and most extensive global satellite sounding records, and it continues to observe the atmosphere for years to come. Our next step of work will be based on the extensive HIRS record to construct a long-term time series of the global temperature and water vapor at different levels of the atmosphere.

5. REFERENCES

Bates, J. J. and D. L. Jackson, 2001: Trands in upper-tropospheric humidity. *Geophys. Res. Letters,* **28**, 1695-1698.

Bates, J. J., D. L. Jackson, F.-M. Breon, and Z. D. Bergen, 2001: Variability of tropical upper tropospheric humidity 1979-1998. *J. Geophys. Res.*, **106**, 32371-32281.

Chevallier, F., 2001: Sampled databases of 60-level atmospheric profiles from the ECMWF analyses. Research Report No. 4, EUMETSAT/ECMWF SAF programme.

Garand, L., D. S. Turner, M. Larocque, J. Bates, S. Boukabara, P. Brunel, F. Chevallier, G. Deblonde, R. Engelen, M. Hollingshead, D. Jackson, G. Jedlovec, J. Joiner, T. Kleespies, D. S. McKague, L. MaMillin, J.-L. Moncet, J. R. Pardo, P. L. Rayer, E. Salathe, R. Saunders, N. A. Scott, P. Van Delst, and H. Woolf, 2001: Radiance and Jacovian intercomparison of radiative transfer models applied to HIRS and AMSU channels. *J. Geophys. Res.*, **106**, 24017-24031.

Jackson, D. L. and J. J. Bates, 2001: Climate analysis with the 21-yr HIRS Pathfinder Radiance clear-sky data set. Proc. 11th Conference on Satellite Meteorology and Oceanography, October 15-18, Madison, WI, 138-140.

Saunders R.W., M. Matricardi and P. Brunel, 1999: An improved fast radiative transfer model for assimilation of satellite radiance observations, *Q. J. Royal Meteorol. Soc.*, **125**, 1407-1426.

Shi, L., 2001: Retrieval of atmospheric temperature profiles from AMSU-A measurement using a neural network approach. *J. Atmos. Ocean. Tech.*, **18**, 340-347.